Sixth International Symposium on Marine Propulsors
smp'19, Rome, Italy, May 2019

Numerical Study of Hull Pressure Fluctuation with Energy Saving Device PSV*

Shucheng Zhai[1], Dengcheng Liu[1], Yongbo Hang[1,2]

[1]China Ship Scientific and Research Center, National Key Laboratory of Ship Vibration and Noise, Wuxi, Jiangsu, China

[2]CSIC Shanghai Marine Energy Saving Technology Development Co., Ltd., Shanghai, China

ABSTRACT

The numerical prediction method of the propeller cavitation and hull pressure fluctuation in the ship stern is set up in the paper using unsteady viscous RANS approach and Schnerr-Sauer cavitation model. Firstly, we predict the hull pressure fluctuation induced by propeller without Pre-Shrouded Vanes (PSV,CMES-PSV®), and the simulations are verified by experimental results. Then the numerical method is used to study the hull pressure fluctuation with PSV, which has five fins and half duct. The cavitation shape and the amplitudes of the first and second blade frequency (BF) of hull pressure fluctuation are compared. When use PSV energy saving device, the 1BF and 2BF pressure fluctuation decrease about 33% and 20% respectively, and the cavitation shape area also decrease.

Keywords

propeller cavitation, CFD, pressure fluctuation, energy saving device.

1 INTRODUCTION

The viscous RANS approach has been used for the flow simulation around propeller widely since 1980s, the early work of cavitation simulation targets hydrofoil and underwater vehicle, and has been accomplished mainly by commercial CFD solvers. As one important aspect of propeller performance, the propeller cavitation has been studied by numerical simulation method, and some research papers come in public. Da-Qing Li (2012) has predicted the E779A cavitation in non-uniform wake based on RANS approach and Zwart cavitation model using ANSYS FLUENT. Kwang-Jun Paik (2013) has predicted the propeller cavitation pattern and the hull pressure fluctuation induced, using FLUENT and Schnerr-Sauer cavitation model.

With the more and more energy saving devices installing in ship stern, the propeller cavitation and hull vibration risk increase. On this condition, we should evaluate the hull pressure fluctuation and cavitation when the energy saving device fixed in ship stern.

The present work aims to compare the unsteady propeller cavitation in the stern region with and without PSV, with special attention to the unsteady cavitation behavior and the vibration risk.

2 NUMERICAL METHODS AND MODELS

2.1 Governing equations

The unsteady RANS approach is adopted because of the significantly lower computational effort than LES.

$$\frac{\partial \rho}{\partial t}+\nabla\left(\rho U\right)=0 \tag{1}$$

$$\frac{\partial \rho U}{\partial t}+U\bullet\nabla\left(\rho U\right)=\nabla\bullet\left(\left(\mu+\mu_t\right)\nabla U\right)-\nabla p-F_s \tag{2}$$

The turbulent viscosity μ_t is modeled by the SST κ-ω turbulence model together with wall functions.

In the VOF approach, the physical properties of the fluid are scaled by the liquid volume fraction γ, with γ=1 corresponding to pure water.

The density and dynamic viscosity of the fluid are scaled as

$$\rho=\gamma\rho_l+\left(1-\gamma\right)\rho_v \tag{3}$$

$$\mu=\gamma\mu_t+\left(1-\gamma\right)\mu_v \tag{4}$$

The mass transfer equation of the liquid volume fraction γ can be written as

$$\frac{D\gamma}{Dt}=\frac{\partial}{\partial t}+\nabla\bullet\left(\gamma U\right)=\frac{\dot{m}}{\rho_l} \tag{5}$$

where the mass transfer rate $\dot{m}$ is to be modeled by cavitation models.

* Corresponding author, E-mail: zsc_cssrc@163.com.

Project supported by the National Natural Science Foundation of China (Nos.11102188 and 91852101)

The transport Equation (1) for mass (continuity equation) can be re-written in combination with Equation (1), Equation (3) and Equation (5).

$$\nabla \bullet \mathrm{U} = \dot{m}\left(\frac{1}{\rho_l} - \frac{1}{\rho_v}\right) \tag{6}$$

It implies that the cavitation model is involved in the coupling procedure of velocity and pressure. For the cavitation flow simulations, the sources of the mass transfer equation are computed in the PISO loop firstly, then the volume fraction transport of the vapour is progressed, and the standard PISO procedure is entered.

2.2 Cavitation model

Cavitation is the transition of liquid into vapour in the low pressure regions caused by the presence of small gas nuclei in the fluid. The Schnerr-Sauer cavitation mass transfer model is employed to mimic the phase change between vapour and liquid,

$$\dot{m} = sign\left(p_v - p\right)\frac{n_0}{1 + n_0 \frac{4}{3}\pi R^3} 4\pi R^2 \sqrt{\frac{2}{3}\frac{|p_v - p|}{\rho_l}} \tag{7}$$

where n_0 stands for the number density of micro bubbles per liquid volume and R is the initial nuclei radius. Schnerr-Sauer's model is based on bubble dynamics by considering the equation of motion of a single bubble of radius R.

2.3 Discretization and solution procedure

The finite volume method is used for the discretization of the governing equations, and the unsolved flow variables are stored in the cell-center positions in the computational grid. The Euler differencing scheme is used for the time discretization, and a second order differencing scheme is adopted for the components of the momentum equation.

The commercial solver Fluent 6.3 used in this study is a multiphase solver，taking two fluids into account using the VOF method.

To improve the convergence of the cavitation flow and reduce the computational time, the full wetted flow is simulated using MRF method at first, after obtaining a quasi-stable flow field, the sliding mesh is then applied to simulate the rotation of propeller. The three components of the momentum equation are solved sequentially in a loop within each time step. The PIMPLE algorithm is applied for the coupling between the velocity and the pressure fields, allowing for stable transient simulations with max C_o>1. The PIMPLE algorithm is a combination of the SIMPLE and PISO algorithms, where the PISO loop is complemented by an outer iteration loop and the under-relaxation of the variables.

3 BOUNDARY CONDITIONS AND MESH GENERATION

The configuration investigated here is a tanker, which is a single screw vessel, driven by a fixed pitch four-bladed propeller. The principle parameters of model propeller is provided in Table 1, and the hull and propeller are visualized in Figure 1.

Table 1 The principle parameters of model

Length of waterline, L_{WL}	6.503
Breadth, B	1.119
Draught, T	8.5
Propeller diameter, D	0.216
Number of blades , Z	4
Expanded area ratio	0.38
Pitch ratio	0.78

Figure 1 The bulk tanker and propeller model

The inlet boundary is defined as velocity inlet condition with a fixed value of velocity U. The outlet boundary defined as pressure outlet condition, and the pressure value is constant based on the cavitation number σ_n. The hull, propeller, PSV, rudder and hub boundary are defined as no-slip wall conditions, respectively.

The mesh is generated using HEXPRESS. The computational domain is divided into two sub-regions. The ship region contains the flow region that includes the inlet, outlet, ship, PSV and rudder, the propeller region is a small cylinder surrounding the propeller. The grid of the two sub-regions all consist of unstructured hexahedral cells, and a number of the boundary layer cells are inserted, the non-dimensional parameter of the hull, $y^+ \approx 100$. The ship region and propeller region are consist of 5.51 million and 1.01 million cells, respectively. The overview of surface mesh is shown in Figure 2.

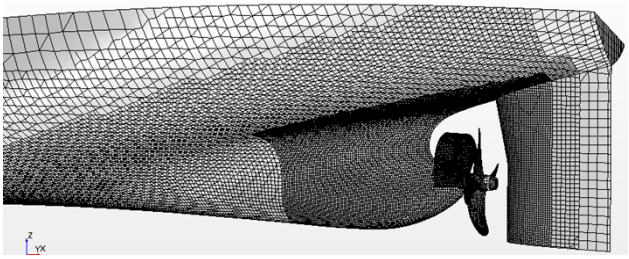

Figure 2 Surface mesh of stern region

4 RESULTS AND DISCUSSIONS

4.1 Method validation

The method to predict the cavity and hull pressure fluctuation was checked by experimental results of a container ship. The experiment of cavitation observation and measurement for the model propeller is performed in the large cavitation channel of China Ship Scientific Research Center. Figure 2 and Figure 3 is the pressure fluctuation comparison and Figure 4 is the cavitation pattern verification. Through comparison of simulations with experiments, the cavity prediction method is considered reliable and has certain precision.

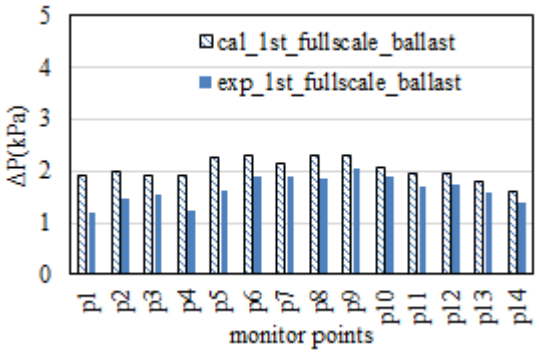

Figure 3 The 1BF of hull pressure fluctuation, calculation vs. experiment

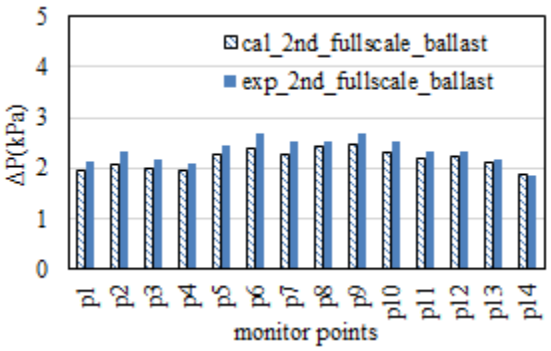

Figure 4 The 2BF of hull pressure fluctuation, calculation vs. experiment

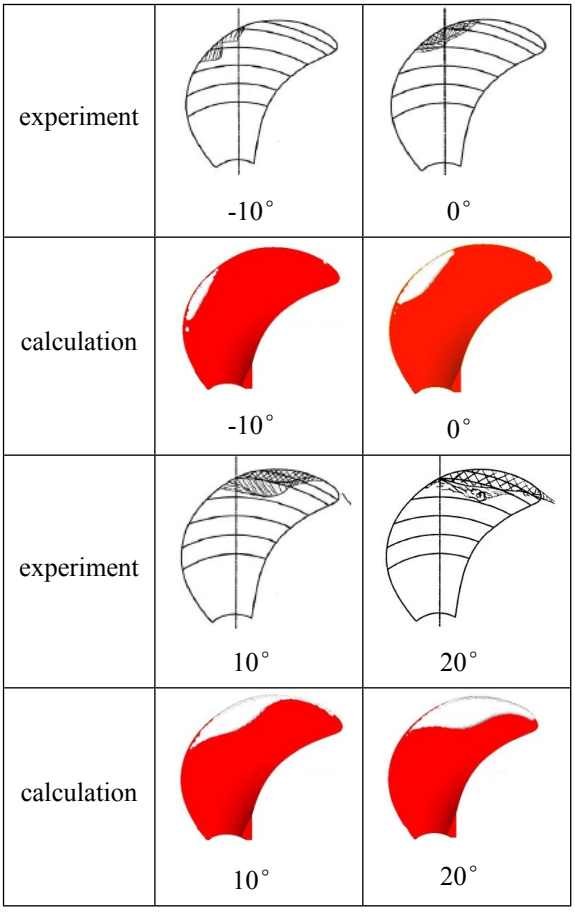

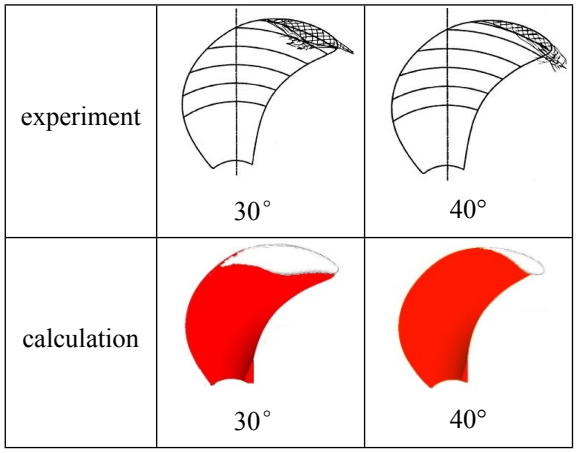

Figure 5 The cavitation sketches at ballast draft condition, calculation vs. experiment(model scale)

4.2 Comparison and Analysis

The test conditions of the cavitation observation and measurement in this study are summarized in Table 2.

Table 2 The test conditions

	Ballast draft with/without PSV
n	7.462
$\sigma_{n0.8R}$	0.336
K_T	0.1496

where n is the rotational speed of the propeller, $\sigma_{n0.8R}$ is the cavitation number, and K_T is the thrust coefficient. The definitions are as follows:

$$\sigma_{n0.8R} = \frac{p - p_v}{0.5\rho\left(0.8\pi nD\right)^2}$$

$$K_T = \frac{T}{\rho n^2 D^4}$$

The ballast condition is considered by K_T-identity method and adjustment of the channel pressure to the corresponding cavitation number. Firstly, the steady full wetted flow is simulated using MRF method to obtain a quasi-stable flow field, then the unsteady computation is started to simulate the rotation of propeller using sliding mesh method, and the cavitation model is activated to predict the cavitation, finally. The parameters in Schnerr-Sauer cavitation model are selected as n_0=2×10^8, d_{Nuc}=1×10^{-4}.

The main PSV's energy saving mechanism is to reduce the loss of swirl energy of propeller. Figure 7 to Figure 9 is the tangential velocity before propeller. As shown in pictures, when PSV fixed, the tangential velocity changed little because the flow field is upstream. Figure 10 to Figure 12 show the flow field after propeller, from 0.7R to 0.9R, the tangential velocity line of PSV move down, and velocity peak decreases. The PSV creates rotational flow in the opposite direction, which means to reduce the loss of swirl energy of propeller may be attached.

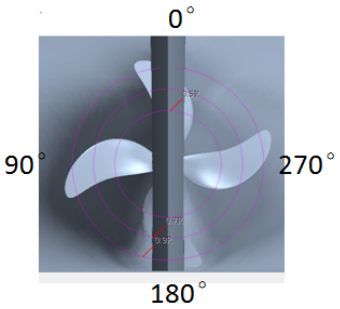

Figure 6 The sketch of degree

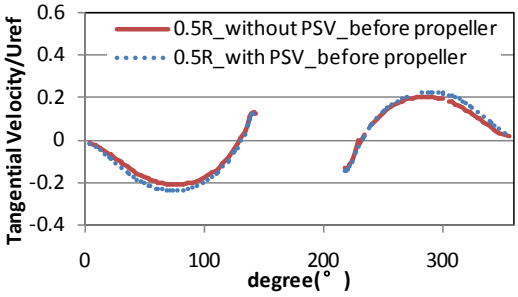

Figure 7 The Tangential velocity before propeller of 0.5R

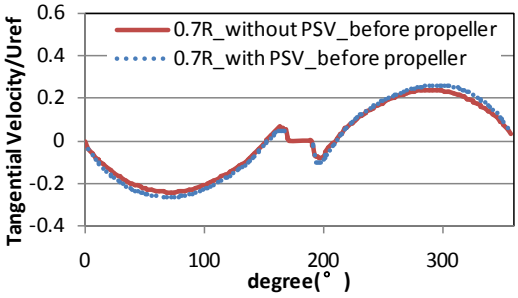

Figure 8 The Tangential velocity before propeller of 0.7R

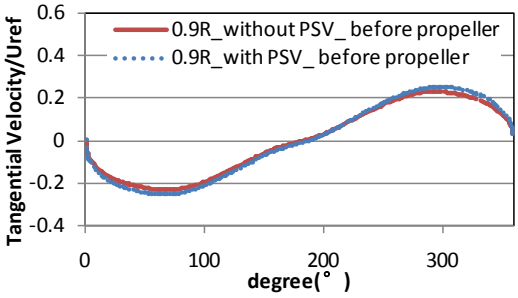

Figure 9 The Tangential velocity before propeller of 0.9R

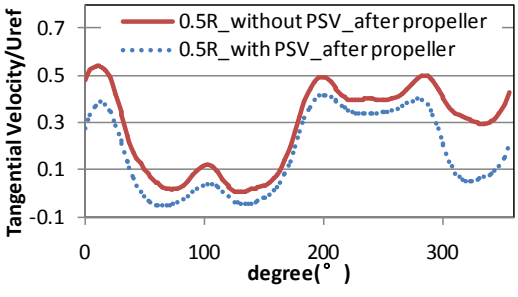

Figure 10 The Tangential velocity after propeller of 0.5R

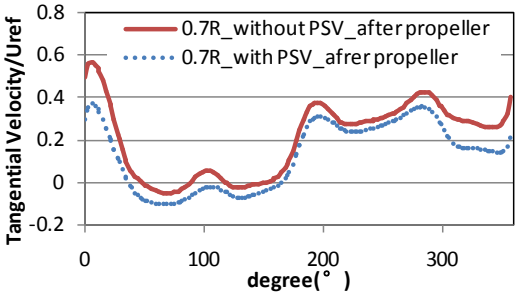

Figure 11 The Tangential velocity after propeller of 0.7R

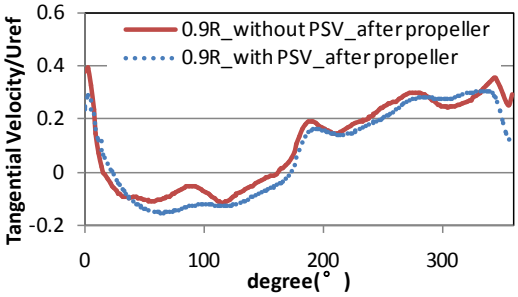

Figure 12 The Tangential velocity after propeller of 0.9R

The self-propulsion point was obtained from the load-varying tests that employ the results from two propeller speeds. The rate of viscous resistance (ΔR_m), propeller rotating speed (Δn_m), and delivered power (ΔP_{Dm}) at self-propulsion point are indicated in Table 3. The rate refers to the value as compared with the results from the bare hull without PSV.

Table 3 Rates of viscous resistance, propeller rotative speed and delivered power of PSV (model scale)

	ΔR_m(N)	Δn_m(%)	ΔP_{Dm}(%)
With PSV	1.201	-3.2%	-3.3%

The predicted cavitations in the stern region at ballast draft with and without PSV is compared in Figure 13 and Figure 14, respectively.

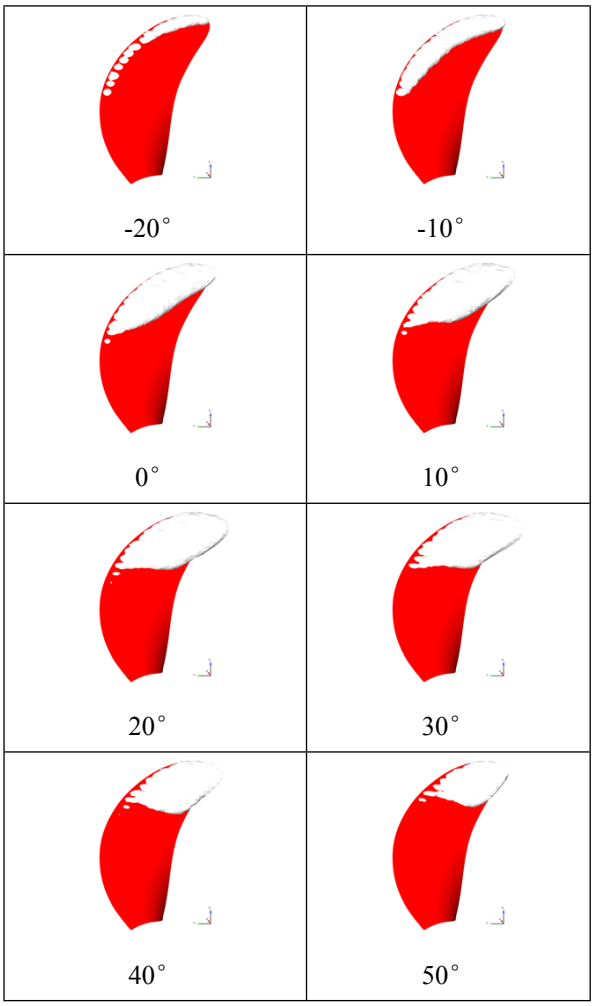

Figure 13 The simulation sketches at ballast draft condition without PSV (model scale)

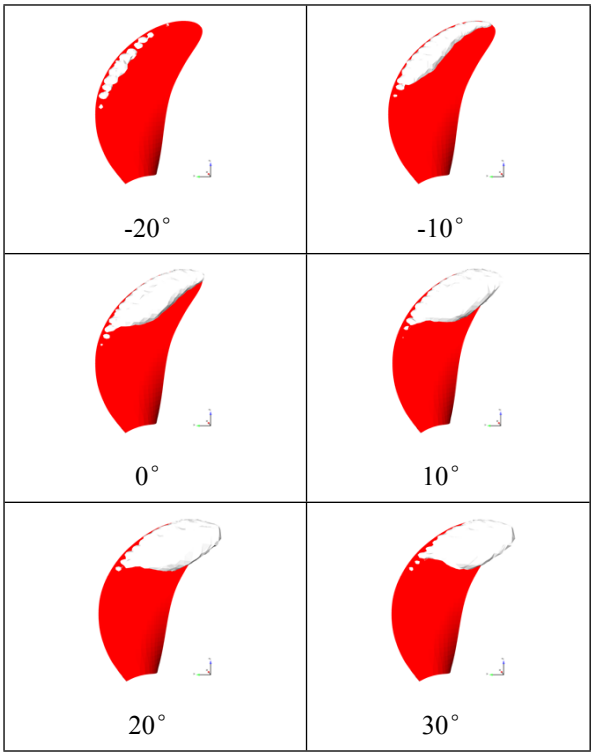

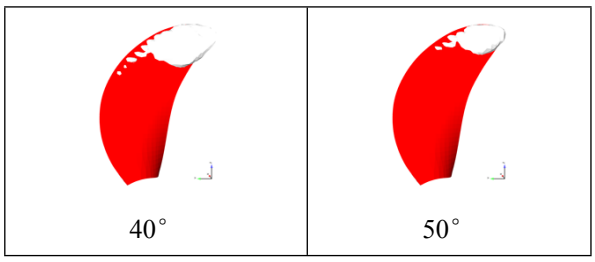

Figure 14 The simulation sketches at ballast draft condition with PSV(model scale)

In Figure 16 and Figure 17, the predicted cavity, represented by vapor iso-surface of 0.1 shows the same different. The key feature, the extent change of the attached cavity with the rotation angels and the collapse at the tail of the main cavity shows almost the same. The cavity begins at about the same location φ=-20º, reaches the maximum area at φ=20º at ballast draft condition. At each position, the cavity sketch without PSV is a little larger than with PSV.

In order to investigate the hull pressure fluctuation induced by cavitation, the monitor points are arranged on the stern surface shown in Figure 15.

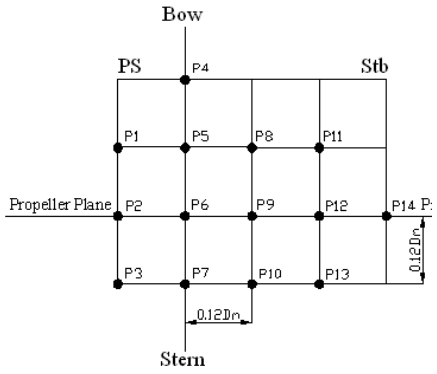

Figure 15 The arrangement of monitor points

The pressure fluctuation predicted at model scale is analysed by FFT, and converted to the pressure fluctuation at full scale by the formula. The amplitudes of the first blade frequency (1BF) of the hull pressure fluctuation predicted at ballast draft condition is compared with and without PSV in Figure 16 and Figure17. When use PSV energy saving device, the 1BF and 2BF pressure fluctuation decrease about 33% and 20% respectively. At most time, the cavitation the hull pressure fluctuation should be checked when fixed PSV, to make sure there is no cavitation erosion and vibration risk. In this case, the pressure fluctuation and cavitation shape have been improved when installing PSV.

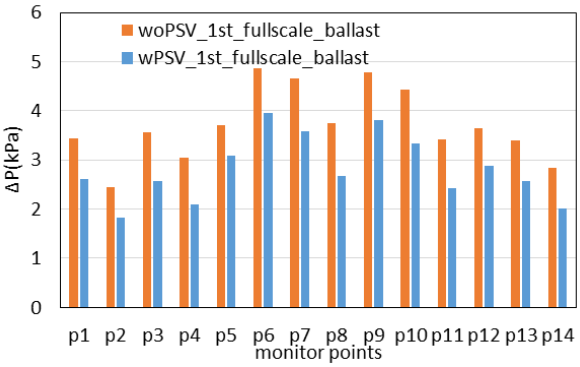

Figure 16 The 1BF of hull pressure fluctuation predicted with and without PSV

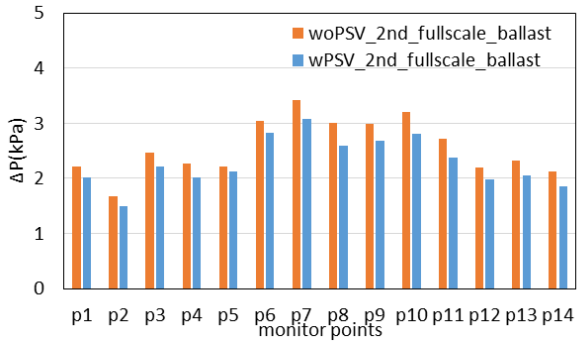

Figure 17 The 2BF of hull pressure fluctuation predicted with and without PSV draft condition

5 CONCLUSIONS

In this paper, the propeller cavitation shape and the amplitude of the first blade frequency (1BF) and the second blade frequency (2BF) with and without PSV are predicted. Firstly, the simulation method is checked. The prediction results show good agreement with test results. Then the cavitation character of target ship model is simulated by this method. The hull pressure fluctuations decrease when install PSV, and at each position, the cavity pattern without PSV is a little larger than with PSV. Therefore, when we install this energy saving device to ship, there is no cavitation erosion and vibration risk.

REFERENCES

TANG D H, CHEN J D, ZHOU W X. (1998) . 'Comparative calculationsof propeller performance by RANS/Panel Menthod'. 22nd ITTC Propulsion Committee Propeller RANS/Panel Method Workshop, Grenble

CHEN J D, ZHOU W X, TANG D H, et al. (1998) .'Comparative calculations of unsteady propeller performance by panel menthod'. 22nd ITTC Propulsion Committee Propeller RANS/Panel Method Workshop, Grenble

Da-Qing Li. (2012) . 'Prediction of Cavitation for the INSEAN Propeller E779A Operating in Uniform Flow and Non-Uniform Wakes'. 8th International Symposium on Cavitation, Singapore, pp.368-373

Kwang-Jun Paik. (2013) . 'URANS Simulations of Cavitation and Hull Pressure Fluctuation for Marine Propeller with Hull Interaction'. 3nd International Symposium on Marine Propulsors, Tasmania, pp.389-396

Abolfazl Asnaghi. (2015) . 'Computational Analysis of Cavitating Marine Propeller Performance using OpenFOAM'. 4th International Symposium on Marine Propulsors, Tesas, pp.148-155

Rickard E Bensow. (2015) . 'Large Eddy Simulation of a Cavitating Propeller Operating in Behind Conditions with and without Pre-Swirl Stators'. 4th International Symposium on Marine Propulsors, Tesas, pp.458-477

Zheng Chaosheng. (2016) . 'The unsteady numerical